Measurement of Double Differential Cross Sections of Charged Particle Emission Reactions for ^{nat}Zr, ^{27}Al and ^{nat}Ti by Incident DT Neutrons

Hiroyuki Takagi, Kokooo, Isao Murata, Akito Takahashi
Department of Nuclear Engineering, Osaka University
Yamadaoka 2-1, Suita, Osaka, 565-0871, Japan
E-mail: takagi@newjapan.nucl.eng.osaka-u.ac.jp

The double differential cross sections of ^{nat}Zr(n,xp), ^{27}Al(n,xp), ^{27}Al(n,xα), ^{nat}Ti(n,xp) and ^{nat}Ti(n,xα) reactions have been measured by E-TOF two-dimensional analysis method. The measured data were compared with other experimental data, evaluated nuclear data of JENDL fusion-file and theoretical calculation results by SINCROS-Ⅱ.

1.Introduction

Double differential cross sections (DDXs) of charged particle emission reactions induced by incident DT neutrons are important for the evaluation of nuclear heating and material damages in fusion reactor design. However, until now only a few data have been measured because of experimental difficulties, such as very large background and low counting rates. Li_2ZrO_3, $LiAlO_2$ and Li_2TiO_3 can be considered to use as solid breeder material in fusion power reactors because of their inherent advantages, e.g., chemical stability at high temperature, compatibility with structural materials, good tritium recovery characteristics and so on [1]. Thus, the fusion neutronics benchmark experiments have been done for various materials including these breeder materials, low-activation elements and so on at FNS in JAERI [2]. In connecting with these experiments, DDXs of ^{nat}Zr(n,xp), ^{27}Al(n,xp), ^{27}Al(n,xα), ^{nat}Ti(n,xp) and ^{nat}Ti(n,xα) reactions induced by incident DT neutrons have been measured at OKTAVIAN in Osaka University.

2. Experimental procedure

Experiments were carried out by using the charged particle spectrometer based on the two dimensional analysis of energy and time-of-flight of emitted charged particle [3]. The schematic arrangement of the spectrometer is shown in Fig. 1. The spectrometer was located in a vacuum chamber of 1mφ×1m long. The chamber was evacuated to keep a pressure of about 1.3 Pa. The shield assembly made of iron, polyethylene and lead reduced the backgrounds. The CsI(Tl) scintillator, 2mm in thickness and 50mm in diameter, was used as a charged particle detector. The tritium target of pulsed neutron source was positioned in a through tube of the chamber and out of vacuum. The spectrometer can be used to measure the DDX data for emission angles between 30° and 135° . The flight path of emitted particle varies from 30.8 cm to 56.7 cm according to change of the emission angle. The sample

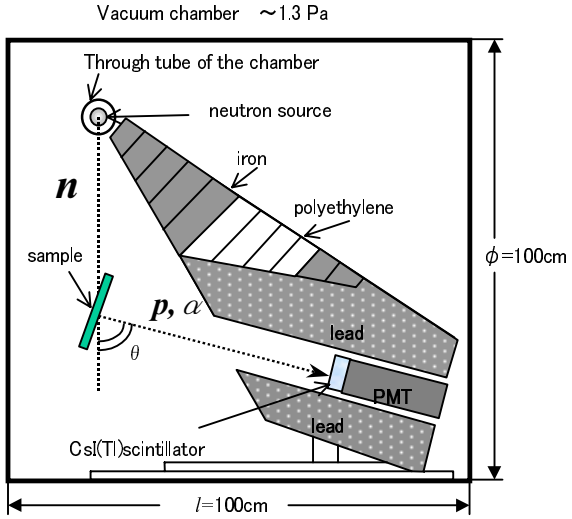

Fig.1 Schematic arrangement of the charged particle spectrometer.

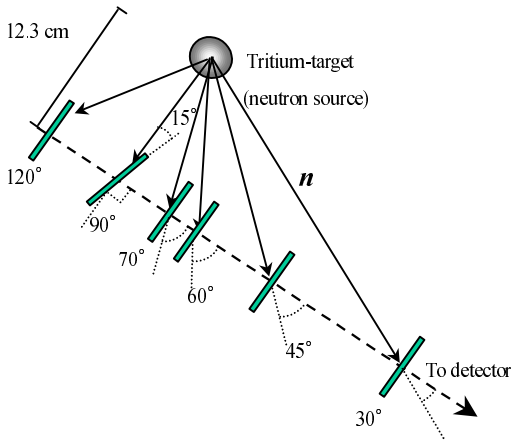

Fig. 2 Sample position for various emission angles.

position for various scattering angles can be seen in Fig. 2.

The block diagram of the measuring system is shown in Fig. 3. The two dimensional data acquisition has been done by using the pulse-height of dynode signal corresponding to energy and the time-of-flight signal made from the anode signal as start and the beam pick-up ring signal (with delay) as stop. The logic signal created by pulse-shape discrimination (PSD) circuit has been used as the gate signal for E-TOF two-dimensional acquisition. The details about the E-TOF measurement are described in Ref. [3]. An NE213 scintillator is used as a relative neutron flux monitor. In this experiment, thin foil samples of zirconium, aluminum and titanium were employed. The details of the samples are shown in Table 1.

The reason why the CsI(Tl) detector was chosen is its typical property of pulse-shape discrimination. Fig. 4 shows an example of two-dimensional distribution of energy and rise-time for α-particle, proton and γ-ray, by

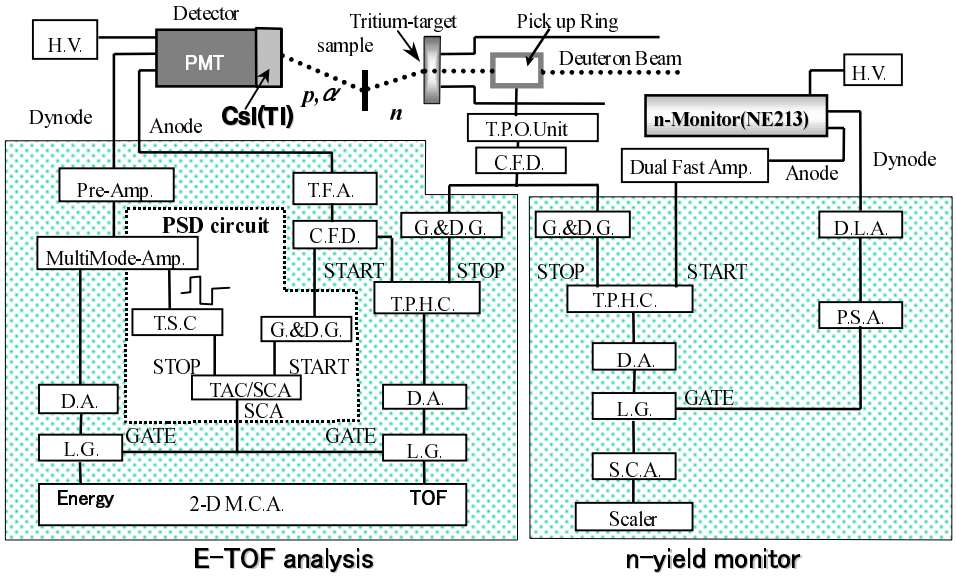

Fig. 3 Block diagram of the measuring system.

using CsI(Tl) detector. The proton reference source was obtained by bombarding the polyethylene sample by DT neutrons. The ^{241}Am standard source was used as α reference. As shown in the figure, the contours of each particle signals were separated each other. Thus, we can choose either α-particle or proton signal by this technique. However, there still exist background counts by the charged particles produced in the surrounding structural materials, such as through tube, vacuum chamber, shield assembly and so on. So, an additional technique, namely the two-dimensional E-TOF analysis for charged particles, was applied. It is based on the following equation,

Table 1 The dimension of the samples.

Sample	Measured particle	Φ [cm]	Thickness [μm]	Isotopes (abundance)[%]
^{nat}Zr	*proton*	6.0	25.0	^{90}Zr 51.453 ^{91}Zr 11.224 ^{92}Zr 17.152 ^{94}Zr 17.384
^{27}Al	*proton*	6.0	25.0	^{27}Al 100.00
	α-particle		10.0	
^{nat}Ti	*proton*	6.0	20.0	^{46}Ti 8.25 ^{47}Ti 7.44 ^{48}Ti 73.22 ^{49}Ti 5.41 ^{50}Ti 5.18
	α-particle		10.0	

$$T = F_p \sqrt{\frac{M}{2E}}, \quad (1)$$

where, T is the time-of-flight, F_p the flight path length, and E and M the energy and mass of the particle, respectively. According to this equation, measurement of charged particles produced in samples was achieved successfully.

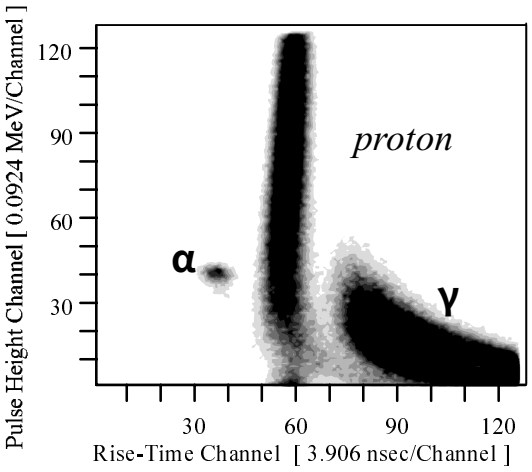

Fig. 4 Two-dimensional distribution of rise time and pulse height spectrum.

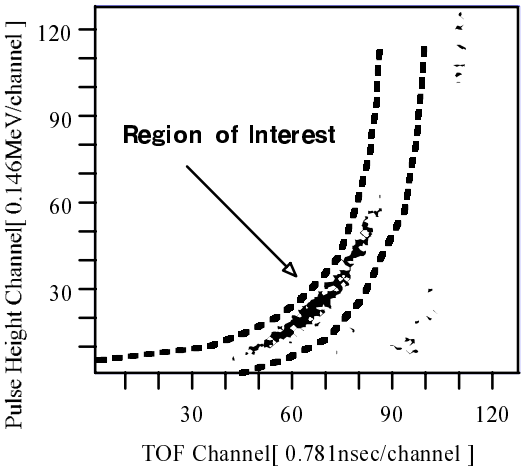

Fig.5 Measured E-TOF spectrum from 27-Al(n,x α) reaction at the emission angle of 60 degree.

3. Data analysis

The net raw data were obtained by subtracting the data in background run from that of foreground run. The background run was undertaken without sample. In Fig. 5, the net raw data spectrum of α-particle from ^{27}Al(n,x α) reaction at the emission angle of 60° is shown as an example. The integral counts of respective charged particle, i.e., proton and α-particle, for each pulse-height channel, namely the net energy spectrum, have been obtained by properly choosing the region of interest within the corresponding contour of E-TOF spectrum.

In this experiments, the lower-energy thresholds of proton and α-particle measurements were 2.5 MeV and 3 MeV, respectively.

To obtain absolute DDX, $\sigma(E,\theta)$ barn/sr/MeV, the net energy spectrum was normalized by comparing the value of angular differential cross section (ADX) of evaluated nuclear data files for recoil proton from H(n,p) reaction with the yield of recoil proton obtained by measurement of thin polyethylene sample [3].

The raw data must be corrected because the broadening functions of angular resolution and the energy loss of the charged particle in the sample are not negligible. The Monte-Carlo simulation calculations with the JENDL-FF cross section data and Bethe-Bloch formula were used to obtain the correction factors for every angle point.

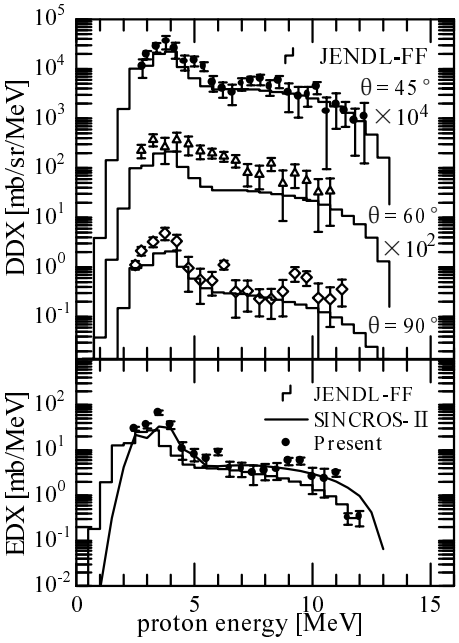

Fig.6 The DDX and EDX data of Zr(n,xp) reaction.

4. Results and discussions

The EDXs and total cross sections were deduced by using the measured DDXs. The measured data were compared with other experimental results, JENDL-FF and SINCROS-II calculation. In SINCROS- II calculations, the normalization factors were determined by comparing the calculated EDX data for neutron emission reaction with the measured data of Takahashi [4,5] for the same nuclides. The experimental results and discussion are described in the following in detail. The comparisons of the total cross sections among the measured data, JENDL-FF and other experimental results are summarized in Table. 2.

4.1. Zirconium

The measurements of proton emission DDXs have been done for three emission angles, i.e., 45, 60, and 90 degrees. The measured DDX and EDX data are shown in Fig. 6. The measured EDX data are larger than the JENDL-FF and SINCROS- II calculations mainly in the energy region between 2 to 4 MeV and 9 to 11 MeV. In the total cross section, the JENDL-FF is largely underestimated.

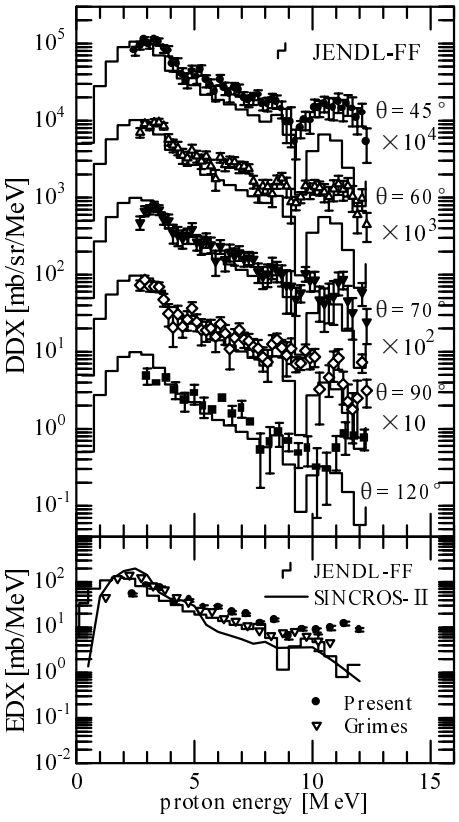

Fig. 7 The DDX and EDX data of Al(n,xp) reaction.

4.2. Aluminum

The DDX data for proton emission reactions were

obtained at the emission angles of 45, 60, 70, 90 and 120° . Fig. 7 shows the measured DDX and EDX data. The present EDX data agree well with other reference data in the energy region between 3 to 5 MeV, while it gives larger data for the energies greater than 5 MeV. In the total cross section, the measured value is smaller than Grimes' data [8] and JENDL-FF, due to low-energy cutoff of this experimental method.

The measured DDX data for α emission reactions at the emission angles of 45, 60, 70, 90 and 120° were provided. In Fig. 8, the measured DDX and EDX data are shown. A fairly good agreement between the present EDX result and JENDL-FF was obtained in the energy region from 4.5 to 9 MeV. However, overestimate of the JENDL-FF is shown in energies lower than 4.5 MeV. For the total cross section, the measured value is slightly smaller than other data.

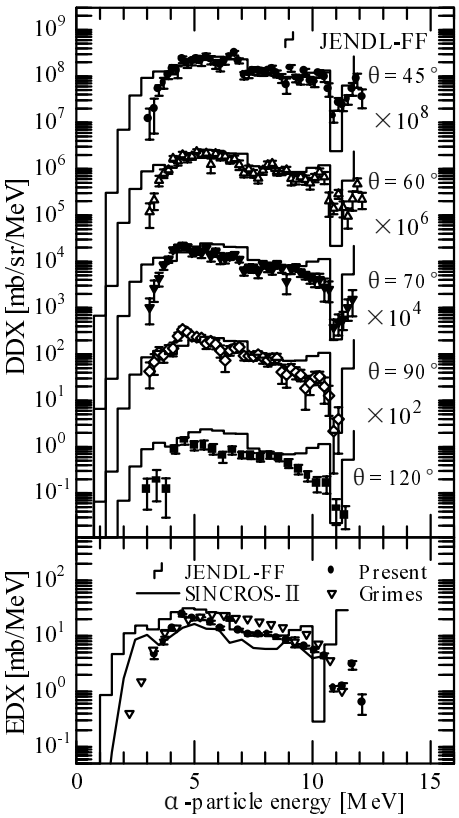

Fig. 8 The DDX and EDX data of Al(n,xα) reaction.

4.3. Titanium

The DDX data of proton emission reactions at emission angles of 60, 70, 90 and 120° were measured. The measured DDX and EDX data are shown in Fig. 9. The JENDL-FF and SINCROS-Ⅱ calculations were smaller than the measured EDX data for energies greater than 7.5 MeV. The total cross section of JENDL-FF is something smaller than the measured data.

The obtained DDX data of α emission reactions at emission angles of 45, 60, 70 and 90° and EDX data are shown in Fig. 10. The measured EDX data were not in agreement with JENDL-FF and SINCROS-Ⅱ calculation. The total cross section of the measured data agrees well with the JENDL-FF.

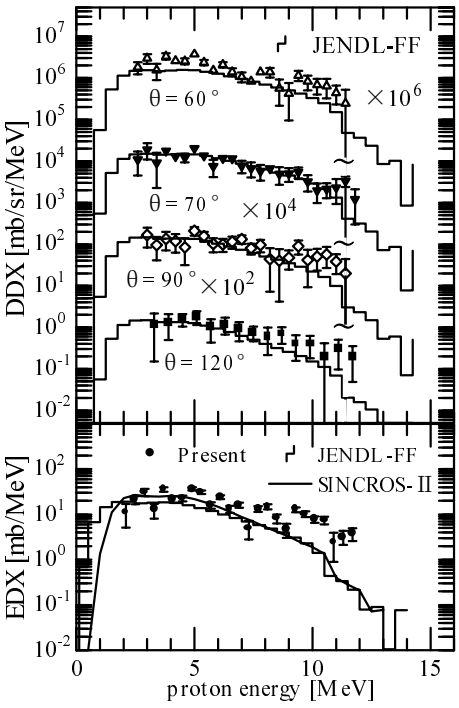

Fig. 9 The DDX and EDX data of Ti(n,xp) reaction.

5. Conclusions

The DDXs of ^{nat}Zr(n,xp), ^{27}Al(n,xp), ^{27}Al(n,xα), ^{nat}Ti(n,xp) and ^{nat}Ti(n,xα) reactions have been measured at the emission angles between 45 to 120° . The measured data were compared with other experimental data, evaluated nuclear data of JENDL-FF and theoretical calculation results by SINCROS-Ⅱ. The JENDL-FF data for ^{nat}Zr(n,xp) reaction is largely underestimated. In DDX and EDX data of ^{27}Al(n,xα) reaction, the disagreement of the

measured data and JENDL-FF is shown in low energy region (<5 MeV). The measured DDX and EDX spectrum for ^{nat}Ti(n,xα) reaction were not in agreement with JENDL-FF and SINCROS-II calculation overall.

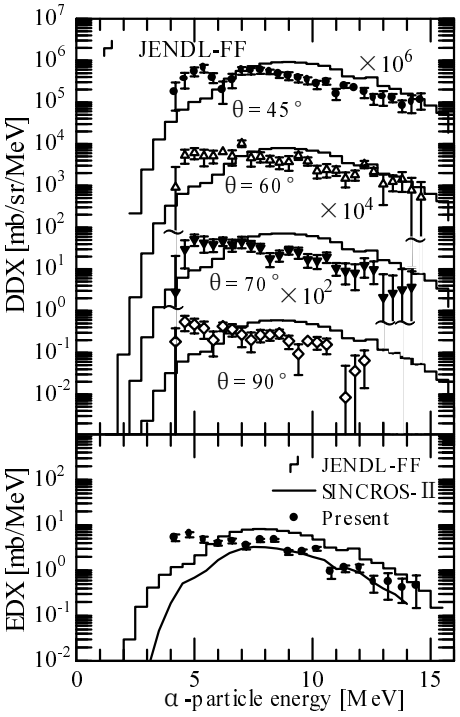

Fig. 10 The DDX and EDX data of Ti(n,xα) reaction

References

[1] Johnson, C. E., *et al.*: "Solid Breeder Materials", *J. Nucl. Mat.*, 103&104, 547 (1981).

[2] Kokooo *et al.*: "Benchmark Experiment on Vanadium Assembly with D-T Neutrons -Leakage Neutron spectrum Measurement-", *Fusion Technol.*, 34, 980 (1998).

[3] Takahashi, A., *et al.*: "A Time-of-Flight Spectrometer with Pulse-Shape Discrimination for the Measurement of Double-Differential Charged-Particle Emission Cross Sections", *Nucl. Instr. Meth.*, A 401, 93 (1997).

[4] Takahashi, A., *et al.*: "Double and Single Differential Neutron Emission Cross Section at 14.1 MeV: Vol.1", *OKTAVIAN Report*, A-87-03, Osaka University, (1987).

[5] Takahashi, A., *et al.*: "Double and Single Differential Neutron Emission Cross Section at 14.1 MeV: Vol.2", *OKTAVIAN Report*, A-92-01, Osaka University, (1992).

[6] Ahn, S. H., *et al.*: "Charged Particles from the 14-MeV Neutron Interaction with Zirconium", *Phys. Rev.*, 119, 1667 (1960).

[7] Armstrong, A. H., *et al.*: "14-MeV (*n*, α) and (*n*,*p*) Cross Sections in Zirconium. II", *Phys. Rev.*, 99, 330 (1955).

[8] Grimes, S. M., *et al.*: "Measurement of Sub-Coulomb-Barrier Charged Particles Emitted from Aluminum and Titanium Bombarded by 15-MeV Neutrons", *Nucl. Sci. Eng.*, 62, 187 (1977).

[9] Kneff, D. W., *et al.*: "Helium Production in Pure Elements, Isotopes, and Alloy Steels by 14.8-MeV Neutrons", *Nucl. Sci. Eng.*, 92, 491 (1986).

Table 2 The measured total cross-sections of charged particle emission reactions compared with JENDL-FF and other experimental results.

Reaction	**Present Work** σ(mb) (E_n = 14.1 MeV)	**JENDL-FF** σ(mb)	**Other experiment** σ(mb)
^{nat}Zr(n,xp)	124.7±6.6	68.5	87±22 (E_n=14 MeV) Ahn [6] 180±70 (E_n=14 MeV) Armstrong [7]
^{27}Al(n,xp)	286.2±5.8	361.4	399±60 (E_n=15 MeV) Grimes [8]
^{27}Al(n,xα)	91.3±1.5	125.2	121±25 (E_n=15 MeV) Grimes [8] 143±7 (E_n=14.8 MeV) Kneff [9]
^{nat}Ti(n,xp)	153.1±6.4	105.4	117.4 (E_n=15 MeV) Grimes [8]
^{nat}Ti(n,xα)	34.8±1.2	39.5	36.1 (E_n=15 MeV) Grimes [8]